

sehr kleinen Wert annehmen kann. Man darf ähnliches auch für Sb erwarten.

Der Deutschen Forschungsgemeinschaft sei an dieser Stelle für die Bereitstellung von Forschungsmitteln gedankt.

¹ D. LAZARUS, Phys. Rev. **93**, 973 [1954].

² A. D. LeCLAIRE, Phil. Mag. **7**, 141 [1962].

³ L. C. R. ALFRED u. N. H. MARCH, Phys. Rev. **103**, 877 [1956].

⁴ A. J. MORTLOCK u. A. H. ROWE, Phil. Mag. **11**, 1157 [1965].

⁵ E. A. OWEN u. E. A. O. ROBERTS, J. Inst. Met. **71**, 240 [1945].

⁶ M. HANSEN u. K. ANDERKO, Constitution of Binary Alloys, New York 1958.

⁷ K. DREYER, CHR. HERZIG u. TH. HEUMANN, Proc. Marstrand Conf., Atomic Transport in Solids and Liquids, Verlag der Zeitschrift für Naturforschung, Tübingen 1971, S. 237.

⁸ H. M. GILDER u. D. LAZARUS, Phys. Rev. **145**, 507 [1966].

⁹ W. MOCK, Phys. Rev. **179**, 663 [1969].

¹⁰ S. J. MAKIN, A. H. ROWE u. A. D. LeCLAIRE, Proc. Phys. Soc. London B **70**, 545 [1957].

¹¹ CHR. HERZIG u. a., in Vorbereitung.

Diffusion of He, Ne, and Ar in Vitreous and Partially Devitrified Germanium Dioxide

W. W. BRANDT, B. RAUCH *, and J. J. WAGNER

Department of Chemistry and Laboratory for Surface Studies
University of Wisconsin-Milwaukee, Milwaukee, Wisconsin 53201

(Z. Naturforsch. **27 a**, 617—623 [1972]; received 16 August 1971)

The diffusion coefficients of He, Ne, and Ar in various samples of GeO₂ and approximate values for the corresponding solubility coefficients were obtained from nonisothermal and isothermal desorption experiments. The data show trends similar to those obtained on fused SiO₂, and are interpreted by assuming that the glasses contain many interstices of different critical dimensions and a variety of diffusion paths corresponding to a range of activation energies. Some annealed and partially devitrified samples were studied and the activation energies of diffusion were found to be relatively high. In a few cases, the measurements were extended into and above the glass transition range ($\sim 570^\circ$); the resulting activation energy and the preexponential factor of the Arrhenius equation for the diffusion coefficient were markedly increased, indicating that the diffusion mechanism is probably drastically changed.

Introduction

Up to now, very little is known about the diffusion rates of small gas molecules in vitreous GeO₂^{1, 2}, one of the important one-component glass forming substances. By contrast, various other physical properties of this glass have been studied^{3–10}, usually in comparison to fused SiO₂, so as to characterize the random network structures present as best this may be possible. Diffusion and solubility measurements might contribute to this overall goal, complementing perhaps some of the ideas and theories concerning glass structure, as will be discussed below.

Vitreous GeO₂ is known to devitrify quite readily at elevated temperatures^{11, 12}, and traditional permeation experiments on very thin membranes of

GeO₂ would therefore probably be extremely difficult, especially under isothermal conditions. Recently, a fairly rapid nonisothermal technique has been developed in this laboratory for the determination of diffusion coefficients¹³. Using this approach, GeO₂ samples need not be exposed to elevated temperatures for very long, and the devitrification can thus be kept within acceptable limits (about 4%). Furthermore, since the glass transition range of GeO₂ (570 °C) can easily be reached and the melt viscosity around 600 °C is very high, one can readily study this substance above as well as below the glass transition, using the nonisothermal method.

The earlier results from the new techniques as applied to fused SiO₂¹³ were found to agree fairly well with literature values derived from isothermal measurements. In the present study, results obtained by

Reprint requests to Dr. W. W. BRANDT, Department of Chemistry, The University of Wisconsin-Milwaukee, Milwaukee, Wisconsin 53201, Area Code - 414, USA.

* Present address: Roehm, G.m.b.H., Darmstadt, West Germany.



Dieses Werk wurde im Jahr 2013 vom Verlag Zeitschrift für Naturforschung in Zusammenarbeit mit der Max-Planck-Gesellschaft zur Förderung der Wissenschaften e.V. digitalisiert und unter folgender Lizenz veröffentlicht: Creative Commons Namensnennung-Keine Bearbeitung 3.0 Deutschland Lizenz.

Zum 01.01.2015 ist eine Anpassung der Lizenzbedingungen (Entfall der Creative Commons Lizenzbedingung „Keine Bearbeitung“) beabsichtigt, um eine Nachnutzung auch im Rahmen zukünftiger wissenschaftlicher Nutzungsformen zu ermöglichen.

This work has been digitalized and published in 2013 by Verlag Zeitschrift für Naturforschung in cooperation with the Max Planck Society for the Advancement of Science under a Creative Commons Attribution-NoDerivs 3.0 Germany License.

On 01.01.2015 it is planned to change the License Conditions (the removal of the Creative Commons License condition "no derivative works"). This is to allow reuse in the area of future scientific usage.

both methods and on similar samples are compared to gain additional support for the use of the non-isothermal method.

Experimental

The germanium dioxide used was Alfa Inorganics Ventron grade, 99.999% pure, except for a small and variable amount of water present. The granular material was either used in its original condition, or it was melted at about 1470° for about one-half hour, broken up, ground, and sieved several times in an atmosphere of 10 to 15% relative humidity. The size distributions of the resulting batches were determined microscopically as described earlier¹³, with the principal results as shown in Table 1. The densities of the original and of the remelted material were found to be 3.81 ± 0.03 g/ml and 3.612 ± 0.004 g/ml, respectively, using a pycnometer with benzene as immersing liquid.

Table 1. Sample characteristics of vitreous GeO₂ samples.

Sample	Melt ^a	Number Average Grain Diameter	Relative Variance ^b
B	a	3.2 mm	0.01
C	b	770 μ	0.045
D	b	510 μ	0.089
E	c	121 μ	0.059
F ^c } G ^c }	d	172 μ	0.083
H	d	$18.0 \pm 3.3 \mu^d$	0.18
I	e	10.4 to 16.2 μ^e	0.34
J	e	14.9 to 20.6 μ^e	0.34
K	d	105 μ	0.083
L	f	1.0 cm	~
M	—	14.0 μ	0.085

^a The melting conditions "a" to "f" differed only little from one case to the next. The commercial Sample M was used as received.

^b The relative variance is calculated as $[\overline{d^2}/(\overline{d})^2] - 1$, where \overline{d} is the average grain diameter, and $\overline{d^2}$ the average of the squared diameters.

^c Samples F and G were portions of a single batch.

^d The random error estimate for the diameter originates from replicate microscopic determinations of the size distribution histogram and is considered typical for all samples listed.

^e The lower estimate of the number average diameter of Samples I and J is based on all particles present while the higher estimate is based only on a fairly distinct group of larger particles present and is considered more appropriate in view of the graphical evaluation method used in this work.

Several small batches of the remelted, ground, and sieved material were annealed between 630° and 890°, for a number of hours, so as to obtain partially devitrified samples.

The X-ray diffraction patterns of the commercial granular material, Sample M, of several remelted samples, and of all annealed samples were obtained on a Jarrell-Ash Model 80-300 diffractometer, using

CuK α radiation. Since perfect crystals were not available, Sample M was used as a relative standard; to determine the crystallinity of this material, the amorphous scatter was measured in the range $2\theta = 47^\circ$ to 56° , where θ is the angle of incidence. This result was corrected for the small background originating from the sample holder material, and compared to the corresponding value of a nearly amorphous sample. Next, from the amorphous content so obtained, the crystallinity of Sample M was calculated by difference. Finally, the crystalline diffraction peak heights of the various other samples were divided by those of Sample M, at $2\theta = 47^\circ$, 52° , and 56° , and their crystallinities estimated indirectly from the average values of these ratios. The results so obtained are listed in Tables 2 and 3, together with the principal experimental results. Only the hexagonal modification of GeO₂ was detected in the samples used; this form is known to form first during devitrification¹⁵. GeO₂ samples of small grain size were found to devitrify readily at high relative humidity, even at room temperature^{2,3}. Presumably this crystallization is confined to the surface of the individual grains and may be very different from that produced by annealing. To minimize changes on the surfaces, the samples were handled and stored at low relative humidities.

The relative amounts of crystalline material present in the annealed samples and in Sample M were also determined from the height of a small sub-maximum of the IR absorbance near 970 cm⁻¹, known to be characteristic of the hexagonal modification of GeO₂¹⁶⁻¹⁹. The absorbance values were actually more reproducible than the X-ray results, and both sets of data showed a linear correlation. The IR measurements based on the KBr pellet method were very convenient and required only very small amounts of sample, but the resulting measures of crystallinity are only relative ones, at this time.

To characterize the GeO₂ samples further, the pore volumes were measured by a mercury intrusion method using a 60,000 psi "Porosimeter" of the American Instrument Company. The results obtained on two typical samples are shown in Figure 1. Also, BET surface areas were determined on a sample of small grain size (Sample M), using Kr as sorbate at liquid nitrogen temperature²⁰. The surface area was found to be 0.46 ± 0.04 m²/g, which is roughly three times larger than the microscopically visible area.

Most of the desorption experiments were done under nonisothermal conditions as described earlier^{13,21}, the sample being heated at a slow and uniform rate. The method is efficient even though the precision achieved in the individual experiments is somewhat lower than what is possible in isothermal desorption experiments, as discussed in detail in the earlier publication¹³.

A number of isothermal runs were performed to check the accuracy of the results. This second method used also has been reviewed earlier¹³, including the internal sensitivity calibration of the mass spectrometer using commercial standard leaks, and the semi-automatic operation of the instrument²².

Table 2. Summary of results from nonisothermal desorption experiments on amorphous and slightly devitrified samples of GeO₂.

Sample ^a	Number of Experiments	Sorption Time [h]	Sorption Temp. [°K]	T_{\max}^b [°K]	ΔT^c [°K]	E^d [kcal/mole]	$\log D_0^{d,e}$
He Experiments							
C	2	16	~ 548	451	162	9.3	- 2.5
D	2	21	~ 473	362	104	9.8	- 1.5
					Averages:	9.5	- 2.0
Ne Experiments, below T_g^h							
B	1	20	~ 673	817	357	13.0	- 2.0
C	1	18	~ 573	690	222	15.3	- 2.1
D	2	12	~ 673	599	201	13.3	- 2.5
E ^f	5	12	~ 673	508	130	14.8	- 2.0
F	2	26	~ 673	530	144	15.3	- 2.0
K ^f	3	15	~ 950	526	130	16.0	- 1.2
H ^f	} small grains	4	~ 608	429	129	11.5	- 4.4
I		21	~ 473	428	104	13.7	- 3.2
J		2	~ 598	412	102	12.9	- 2.4
					Averages:	13.9	- 2.5
Ne Experiments, above T_g^h							
L	1 ^g	14	~ 848	946	271	23.5	1.2
Ar Experiments							
H	1	12	~ 673	799	223	23.4	- 4.1
J	2	15	~ 723	769	292	15.2	- 5.3
					Averages:	17.9	- 4.9

^a Sample characteristics are summarized in Table 1.^b T_{\max} is the temperature at which the desorption rate reached its maximum.^c ΔT is the half-width of the desorption transient curve.^d For definitions, see Equation (1). For detailed description of the method of evaluation, see Ref. ¹³.^e The units of D_0 are cm²/sec.^f The crystallinities of Samples E, K, and H were 3.0, 2.5, and 2.5%, respectively, after the last desorption experiment.^g Several other semi-quantitative results were obtained which confirm this trend.^h T_g is the glass transition temperature of GeO₂.Table 3. Summary of results from nonisothermal experiments on partially devitrified samples of GeO₂ (Samples G, I, and K) and a commercial powder (Sample M).

Sample ^a	Number of Experiments	Sorption Time [h]	Sorption Temp. [°K]	T_{\max}^b [°K]	ΔT^c [°K]	E^d [kcal/mole]	$\log D_0^{d,e}$	x^f [%]
Ne Experiments								
G	2	12	~ 888	919	253	27.6	- 0.6	23
K	3	13	~ 1068	635	179	16.9	- 2.2	12
M [small grains]	2	19	~ 723	931	299	22.1	- 4.9	31
Ar Experiments								
I	1	30	~ 623	849	198	28.1	- 3.0	6

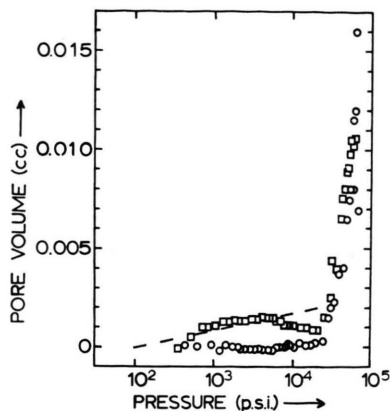
Footnotes a through e can be found at the end of Table 2.

^f Per cent crystallinity, determined by X-ray diffraction methods (see text).

Results

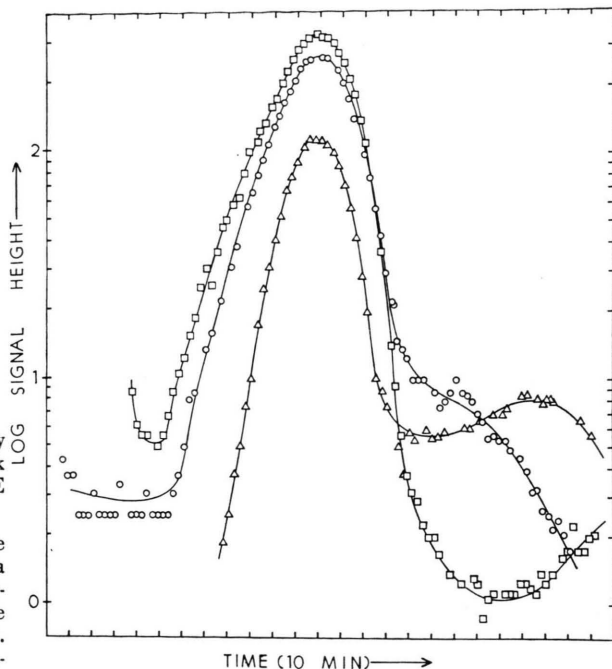
Some typical results from replicate nonisothermal desorption experiments are shown in Figure 2. The small amount of Ne detected early in each run probably constitutes gas left in the interspaces between

the sample grains in spite of repeated rapid flushing of the sample with small portions of an inert gas, such as nitrogen, at the end of the sorption process. The Ne desorbing toward the end of each experiment probably originated from the platinum sheet metal sample containers, judging from blank ex-



↑ Fig. 1. Pore volume as a function of pressure by the mercury intrusion method; dashed line, approximate average blank correction; ○, sample similar to K; □, sample similar to E (see Table 1).

Fig. 2. Typical neon desorption transients obtained on a single sample of GeO_2 , (Sample E). The time scale on the abscissa can be converted to a temperature scale, since a 1 min interval corresponds to a 3.5° rise in temperature. The curves are shifted along the abscissa relative to each other, for clarity. The ordinates are plotted on the same scale. Additional details concerning these runs are given in Table 2. →



periments. The reproducibility of the center part of the curves shown in Fig. 2 is typical of the nonisothermal method.

Some of the GeO_2 granular samples used were sent through an Ar plasma arc in an effort to produce spherical sorbent particles, by quick melting of the surface layer. The desorption transient curves obtained on such samples were quite irregular and non-reproducible in shape, as shown in Fig. 3 (lower curve). The drastic thermal treatment presumably caused the spherical grains to have considerable internal heterogeneity.

Next, in a few cases the desorption experiments were extended into and above the glass transition range and distorted transient curves were obtained as shown in Fig. 3 (upper curve). This result is consistent with the very non-uniform thermal expansion encountered in this temperature range²³.

Finally, some desorption transient curves were obtained on partially devitrified samples (Fig. 4). In general, the temperature where the sorption rates reached a maximum seemed to shift to fairly high values, with increasing crystallinity. Sometimes very irregular desorption curves were obtained which could not be evaluated (see Fig. 4).

From the primary experimental data, that is T_{\max} , the temperature at which the desorption transient

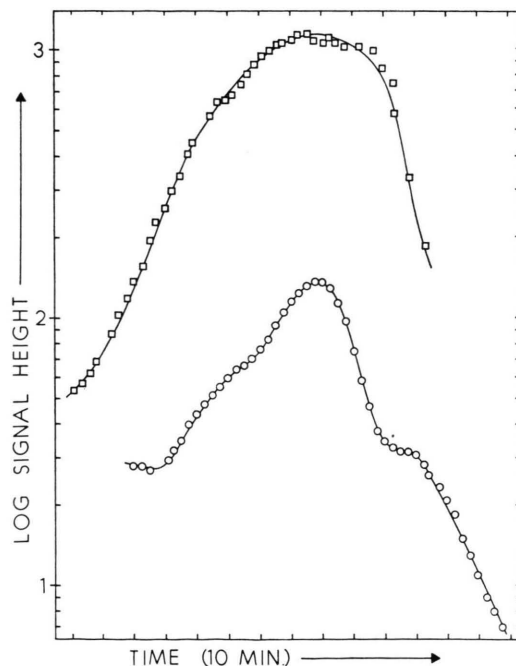


Fig. 3. Distorted desorption transients. □, Sample H, sample entering glass transition range; Ar sorbate. ○, sample superficially melted in a plasma arc, to produce spherical grains (see text). For details on the first experiment, see Table 2. Abscissa and ordinate scales as in Figure 2.

curves reached a maximum, and ΔT , the width of this curve at one-half its maximum height, the parameters E and D_0 were obtained, according to the

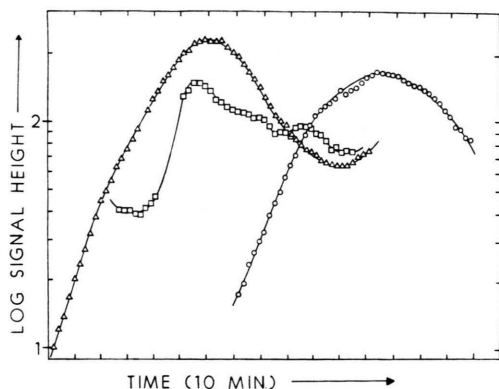


Fig. 4. Neon desorption transients from partially devitrified GeO₂. Δ , Sample K; \square , Sample K devitrified; \circ , Sample G. The different positions of the maxima along the abscissa represent real temperature differences (1 min $\sim 3.5^\circ$), in this case. Additional details on the first and third experiments are given in Table 3. The second experiment was not evaluated due to its very irregular shape. The sample origin and grain size were the same as in the first experiment, and the crystallinity was 22%.

Arrhenius equation for the diffusion coefficient, D , that is

$$D = D_0 \exp\{-E/RT\} \quad (1)$$

where R and T have their usual meaning²¹. The principal results are listed in Tables 2 and 3. The random scatter in the E and D_0 data is distinctly higher than that in the SiO₂ data reported earlier¹³, presumably due to the onset of devitrification; the highly devitrified samples led to results of very low reproducibility (Table 3), consistent with the irregularity of the corresponding desorption transient curves (Fig. 4).

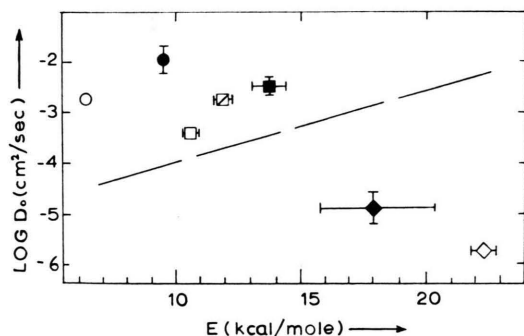


Fig. 5. Logarithm of D_0 (in cm²/sec) plotted against E (in kcal/mole). \circ and \bullet , He in SiO₂ (G.E. Type 151) and in GeO₂, respectively. \square and \blacksquare , Ne in SiO₂ (G.E. Type 151) and in GeO₂, respectively. \diamond and \blacklozenge , Ar in SiO₂ (G.E. Type 151) and in GeO₂, respectively. The dashed line represents the average correlation of literature data mentioned in the text²⁸.

The E and D_0 data reported were corrected for the presence of the grain size distributions in the granular samples, as discussed previously in some detail^{13, 24}. Most corrections for E were smaller than 0.8 (kcal/mole), and for $\log D_0$ smaller than 0.5 units.

The most serious random errors other than those arising from partial devitrification, and from the size distribution are those in ΔT , that is the measured half-widths of the desorption transients; for example, an error of +10 degrees corresponds to +0.6 kcal/mole and +0.16 errors in E and $\log D_0$, respectively, for a typical Ne experiment on Sample I.

The Ar desorption data are distinctly less precise than the He and Ne results because these results reported were obtained on samples of fairly wide size distribution and thus required rather large size distribution corrections¹³, and the minute Ar background present in the mass spectrometer constituted an appreciable fraction of the total Ar present during the desorption experiments.

Some isothermal experiments were carried out to check the above results. The diffusion coefficients obtained are shown in Table 4. The activation energy for Ne in Sample G was found to be 13.2 kcal/mole and $D_0 = 2.5 \times 10^{-4}$ cm²/sec.

Table 4. Summary of results from isothermal desorption experiments.

Sample ^a	Sorption Time [h]	Sorption Temperature [°K]	Desorption Temperature [°K]	$D \times 10^{11}$ ^b [cm ² /sec]
He Experiments				
M (crystal-line)	~ 14	~ 483	483	0.056
M (crystal-line)	~ 14	~ 453	455	0.029
Ne Experiments				
G	12	513	503	5.8
G	12	488	465	1.9
G	12	523	417	0.49
M (crystal-line)	~ 14	~ 483	483	0.0049

^a See Table 1. Sample M is moderately crystalline; sample G is nearly amorphous (not annealed).

^b Graphical method of data evaluation as described in Ref. 13.

To obtain approximate solubilities from the primary rate data, the maximum desorption rate, R_{\max}

[cc(STP)/sec], was determined for each run and multiplied by the half-width of the desorption transient curve, expressed in suitable time units. To obtain R_{\max} , e. g. for a Ne desorption experiment, the following equation was used:

$$R_{\max} = \left(\frac{\text{P.H. (Ne, sample)}_{\max}}{\text{P.H. (Ar, st. leak)}} \right) \cdot \left[\frac{\text{P.H. (Ar, st. leak)}}{\text{P.H. (Ne, st. leak)}} \right] \cdot R(\text{Ne, st. leak}) \quad (2)$$

where $\text{P.H. (Ne, sample)}_{\max}$, $\text{P.H. (Ne, st. leak)}$, and $\text{P.H. (Ar, st. leak)}$ are the measured peak heights of the Ne desorbing at the maximum of the transient curve, that of a Ne standard leak, and that of an Ar standard leak, respectively. $R(\text{Ne, st. leak})$, the rate of Ne flow from the standard leak, was given by the manufacturer (Hastings-Raydist). The first ratio of peak heights was measured during the desorption experiment while the second one, in square brackets, was obtained under similar conditions before and after the experiment. Both ratios are slightly pressure dependent and random errors of 10 or 20% are likely to enter the estimates of R_{\max} , and of the solubilities. The results so obtained are shown in Table 5, together with those for fused SiO_2 , based on earlier data¹³.

Table 5. Approximate solubilities [cc(STP)/g atm] for He, Ne, and Ar in vitreous GeO_2 and SiO_2 .

	GeO_2	SiO_2^a
He	0.8×10^{-2}	1.4×10^{-2}
Ne	0.4×10^{-2}	0.26×10^{-2}
Ar	0.8×10^{-3}	1.6×10^{-3}

^a High purity fused SiO_2 , G.E. Type 151. The Ne solubility in a commercial grade Amersil was found to be 6.1×10^{-3} (same units).

Discussion

The trends in the noble gas solubilities listed in Table 5 probably indicate that relatively large gas atoms find it difficult to penetrate, or to make use of, all the regions of the glass matrix which are accessible to the small He atoms. This result is not very surprising, it is at least qualitatively in agreement with earlier literature data on glasses²⁵, and on zeolites²⁶. By contrast, the solubilities of various gases in organic liquids correlate quite well, e. g. with the Lenard-Jones parameter (ϵ/k), and increase with solute molecular size, indicating that they are controlled in large measure by the sorbent-solute interactions²⁷.

The very strong decrease of the $\log D_0$ values with increasing molecular size may well be related to the differences in accessibility, like the trends in the solubilities. Specifically, the small He atoms may find many useful diffusion paths through the glass random network, while the large Ar atoms cannot penetrate some portions of the matrix. Probably the critical (narrowest) inner dimensions of the interstices used are distributed over a wide range, and a given diffusing gas atom will utilize those passageways which require relatively low activation energies and which are relatively numerous. As a result, there is a balance between the average or measured activation energy and the value of $\log D_0$. Since an independent measure of the number of paths used by a given noble gas atom does not seem available, at this time, it may be fruitless to compare the measured D_0 values to those estimated from absolute rate theory²⁸ or from ZENER's theory²⁹.

The BET surface area of vitreous GeO_2 and the coarse pore volumes determined by the Hg intrusion method are found to be distinctly larger than those of B_2O_3 , a glass of rather low packing density³⁰. Krypton is used as a sorbate in the BET experiments, and the surface area accessible to this gas, at the liquid N_2 temperatures used, seems to be comparatively large, but not descriptive of the deeper lying regions of the glass structure which are accessible to the smaller noble gas atoms at higher temperatures.

In recent years, several attempts have been made to use measured activation energies, E , to estimate a geometrical parameter, r_D , according to a simple expression proposed by FRENKEL^{2, 31, 32},

$$E = 8 \pi G r_D (r - r_D)^2. \quad (3)$$

Here G is the shear modulus of the glass, and r the radius of the diffusing gas atoms. r_D is thought to be the radius of a typical "doorway", the narrowest point of the diffusion path. Several sets of data obtained on amorphous SiO_2 can be readily fitted by this equation, resulting in r_D values between 0.1 Å and 0.3 Å, but the underlying idea that a single type of constrictions or "doorways" control the diffusion of He, Ne, and Ar atoms is not consistent with the distribution of critical dimensions as postulated here. A single value of G is perhaps equally unreasonable.

Rather than pursuing the ideas implicit in Eq. (3), one may regard the E , D_0 , and solubility values reported here and elsewhere as contributing to a more detailed characterization of the glasses studied, on a comparative basis.

As mentioned earlier, the data show a strong and non-uniform dependence of the diffusion parameters D_0 and E on the sample crystallinity. The scatter of the data of Table 3 is rather large, but in general the E values are increased very much on devitrification, while the $\log D_0$ values do not exhibit a consistent trend; $\log D_0$ for Sample M is very low, compared to the other values in this group. Presumably the mode of crystallization and the details of the sample treatment affect the $\log D_0/E$ data very much. From the irregularity of the data (see also Fig. 4) it appears that a simple two-phase model as suggested by Maxwell and as applied to diffusion results

for example by JESCHKE and STUART³³ will not suffice to explain these results.

Finally, the E and D_0 values obtained above the glass transition (Table 2) are very much larger than those found in the lower temperature range. It appears as though a very different mechanism comes into play, perhaps similar to the one(s) suggested for diffusion of gases in organic high polymers³⁴, involving cooperative motions of many degrees of freedom in the vicinity of the diffusing species.

Acknowledgement

The work was supported by the U.S. Atomic Energy Commission under Contract At-(11-1)-1550, and computer funds were furnished by the Laboratory for Surface Studies under a NSF/Departmental Science Development Grant. The authors are indebted to Mrs. SUSAN WAGNER for the IR measurements, and to the colleagues from the General Electric Co., Milwaukee, for the Ar plasma melting experiments.

- ¹ V. G. CANINA and J. DENONCIN, C. R. Acad. Sci. Paris **250**, 1815 [1960].
- ² R. H. DOREMUS, in: Modern Aspects of the Vitreous State, J. D. MACKENZIE, Ed., Butterworths, Washington, D.C., 1962, Vol. 2, p. 1.
- ³ J. D. MACKENZIE in Ref. ², Vol. 1, p. 188.
- ⁴ R. BRUECKNER, (a) Part I, Glastech. Berichte **37**, 413 [1964]; (b) Part II, *ibid.* **37**, 459 [1964]; (c) Part III, *ibid.* **37**, 500 [1964]; (d) Part IV, *ibid.* **37**, 536 [1964].
- ⁵ V. I. DAVYDOV, Germanium, Gordon and Breach, Science Publishers, New York 1966, pp. 144–202.
- ⁶ C. R. KURKJIAN and J. T. KRAUSE, J. Amer. Ceram. Soc. **49**, 134 [1966].
- ⁷ A. NAPOLITANO and P. B. MACEDO, J. Res. Nat. Bur. Stand. **72A**, 425 [1968].
- ⁸ M. HASS, J. Phys. Chem. Solids **31**, 415 [1970].
- ⁹ G. A. FERGUSON and M. HASS, J. Amer. Ceram. Soc. **53**, 111 [1970].
- ¹⁰ J. BLANC, D. BROCHIER, and A. RIBEYRON, Phys. Letters **31A**, 483 [1970].
- ¹¹ V. G. HILL and L. L. Y. CHANG, Amer. Miner. **53**, 1744 [1968].
- ¹² Y. KOTERA and M. YONEMURA, J. Amer. Ceram. Soc. **52**, 210 [1969].
- ¹³ M. ABE, B. RAUCH, and W. W. BRANDT, Z. Naturforsch. **26a**, 997 [1971].
- ¹⁴ P. J. VERGANO and D. R. UHLMANN, Phys. Chem. Glasses **11**, 30 [1970].
- ¹⁵ R. SCHWARZ and W. HASCHKE, Z. Anorg. Chem. **252**, 170 [1943].
- ¹⁶ E. P. MARKIN et al., in: The Structure of Glass, Proceedings of the Third All-Union Conference on the Glassy State, Leningrad 1959, Consultants Bureau, 1960, p. 180.
- ¹⁷ B. H. V. JANAKIRAMA-RAO, J. Amer. Ceram. Soc. **49**, 605 [1966].
- ¹⁸ R. J. BELL, N. F. BIRD, and P. DEAN, Proc. Roy. Soc. London, Solid State Phys., Ser. **2.1**, 299 [1968].
- ¹⁹ E. R. LIPPINCOTT, A. VAN VALKENBURG, C. E. WEIR, and E. N. BUNTINGS, J. Res. Natl. Bur. Stand. **61**, 61 [1958].
- ²⁰ T. J. ADAMS, J. M. SHERWOOD, and F. L. SWINTON, J. Chem. Soc. London A **1195** [1966].
- ²¹ W. W. BRANDT, Int. J. Heat Mass Transfer **13**, 1559 [1970].
- ²² W. W. BRANDT and D. L. DOVALA, Appl Spectr. **23**, 604 [1969].
- ²³ Ref. ^{4b}, Figure 21.
- ²⁴ Ref. ¹³, Table IV.
- ²⁵ R. H. DOREMUS, J. Amer. Ceram. Soc. **49**, 461 [1966].
- ²⁶ G. GNAUCK, E. ROSNER, and E. EICHHORST, Chem. Tech. **22**, 680 [1970].
- ²⁷ J. HILDEBRAND and R. L. SCOTT, Regular Solutions, Prentice Hall, Englewood Cliffs, New Jersey 1962.
- ²⁸ S. GLASSTONE, K. J. LAIDLER, and H. EYRING, The Theory of Rate Processes, McGraw-Hill, New York 1941, pp. 525 et seq.
- ²⁹ C. ZENER, in: Imperfections in Nearly Perfect Crystals, W. SCHOCKLEY, Ed., Wiley, New York 1952, p. 289.
- ³⁰ W. W. BRANDT, T. IKEDA, and Z. A. SCHELLY, Phys. Chem. Glasses **12**, 139 [1971].
- ³¹ K. P. SRIVASTAVA and F. J. ROBERTS, Phys. Chem. Glasses **11**, 21 [1970].
- ³² W. G. PERKINS and D. R. BEGEAL, J. Chem. Phys. **54**, 1683 [1971].
- ³³ D. JESCHKE and H. A. STUART, Z. Naturforsch. **16a**, 37 [1961].
- ³⁴ J. CRANK and G. S. PARK, Diffusion in Polymers, Academic Press, New York 1964, especially Chap. 4.